Cellular/Molecular

Synchronized Bilateral Synaptic Inputs to *Drosophila melanogaster* Neuropeptidergic Rest/Arousal Neurons

Ellena v. McCarthy,[1] Ying Wu,[1] Tagide deCarvalho,[2] Christian Brandt,[3] Guan Cao,[1] and Michael N. Nitabach[1]

[1]Department of Cellular and Molecular Physiology, Department of Genetics, Program in Cellular Neuroscience, Neurodegeneration and Repair, Yale School of Medicine, New Haven, Connecticut 06520, [2]Department of Embryology, Carnegie Institution for Science, Baltimore, Maryland 21218, and [3]Center for Sound Communication, Institute of Biology, University of Southern Denmark, DK-5230 Odense M, Denmark

Neuropeptide PDF (pigment-dispersing factor)-secreting large ventrolateral neurons (lLN$_v$s) in the *Drosophila* brain regulate daily patterns of rest and arousal. These bilateral wake-promoting neurons are light responsive and integrate information from the circadian system, sleep circuits, and light environment. To begin to dissect the synaptic circuitry of the circadian neural network, we performed simultaneous dual whole-cell patch-clamp recordings of pairs of lLN$_v$s. Both ipsilateral and contralateral pairs of lLN$_v$s exhibit synchronous rhythmic membrane activity with a periodicity of ~5–10 s. This rhythmic lLN$_v$ activity is blocked by TTX, voltage-gated sodium blocker, or α-bungarotoxin, nicotinic acetylcholine receptor antagonist, indicating that action potential-dependent cholinergic synaptic connections are required for rhythmic lLN$_v$ activity. Since injecting current into one neuron of the pair had no effect on the membrane activity of the other neuron of the pair, this suggests that the synchrony is attributable to bilateral inputs and not coupling between the pairs of lLN$_v$s. To further elucidate the nature of these synaptic inputs to lLN$_v$s, we blocked or activated a variety of neurotransmitter receptors and measured effects on network activity and ionic conductances. These measurements indicate the lLN$_v$s possess excitatory nicotinic ACh receptors, inhibitory ionotropic GABA$_A$ receptors, and inhibitory ionotropic GluCl (glutamate-gated chloride) receptors. We demonstrate that cholinergic input, but not GABAergic input, is required for synchronous membrane activity, whereas GABA can modulate firing patterns. We conclude that neuropeptidergic lLN$_v$s that control rest and arousal receive synchronous synaptic inputs mediated by ACh.

Introduction

Drosophila melanogaster flies exhibit robust daily rhythms of rest and activity, consisting of two crepuscular bouts of activity with an afternoon siesta in between. This complex daily pattern of activity is generated coordinately by (1) the circadian rhythm control circuit, (2) a homeostatic process regulating sleep, and (3) light input (Cirelli and Bushey, 2008; Dubruille and Emery, 2008; Nitabach and Taghert, 2008).

The *Drosophila* neural circadian control system is comprised of ~150 clock neurons (Renn et al., 1999; Kaneko et al., 2000; Blanchardon et al., 2001; Helfrich-Förster, 2004, 2005; Nitabach and Taghert, 2008). Intercellular communication among timekeeping neurons via neuropeptide signaling and classical neurotransmission is essential for circadian rhythmicity in both insects and mammals (Wagner et al., 1997; Liu and Reppert, 2000; Harmar et al., 2002; Albus et al., 2005; Aton et al., 2005, 2006; Schneider and Stengl, 2005; Maywood et al., 2006; Mertens et al., 2007). The fly large ventrolateral neuron (lLN$_v$) subset of circadian neurons secretes the neuropeptide pigment-dispersing factor (PDF) and their electrical activity has been shown to be directly light-responsive and is modulated by a blue light-activated photopigment called cryptochrome (CRY) (Sheeba et al., 2008a). These neurons are wake-promoting and critical for the regulation of arousal and sleep patterns (Collins et al., 2005; Helfrich-Förster et al., 2007; Parisky et al., 2008; Shang et al., 2008; Sheeba et al., 2008b). The functional signals from these neurons to downstream targets include activity-modulated PDF secretion (Nitabach et al., 2002, 2006; Wu et al., 2008a,b). These functional outputs are modulated by the intrinsic circadian timekeeping mechanism (Cao and Nitabach, 2008), direct activation by light (Sheeba et al., 2008a), and by synaptic inputs, the nature of which are mostly unknown, but likely include GABAergic input (Parisky et al., 2008; Chung et al., 2009).

To begin to unravel the synaptic circuitry of the fly circadian neural network, we used whole-cell patch-clamp physiology in intact whole-brain explants. Simultaneous dual-cell recordings from pairs of lLN$_v$s, regardless of whether they were in ipsilateral or contralateral hemispheres of the brain, revealed highly synchronous rhythmic membrane activity. Rhythmic lLN$_v$ activity is abolished by treating the preparation with either tetrodotoxin (TTX), which blocks action potentials, or α-bungarotoxin or curare, which blocks nicotinic acetylcholine receptors. These data

Received April 20, 2010; revised April 13, 2011; accepted April 14, 2011.

Author contributions: E.v.M., Y.W., G.C., and M.N.N. designed research; E.v.M., Y.W., T.d., C.B., and G.C. performed research; E.v.M. and Y.W. analyzed data; E.v.M., Y.W., and M.N.N. wrote the paper.

This work was supported in part by NINDS–NIH Grants R01NS056443, R01NS055035, and R21NS058330 (laboratory of M.N.N.). Y.W. was supported by NINDS–NIH Ruth L. Kirschstein National Research Service Award (NRSA) Postdoctoral Fellowship F32NS055527. E.v.M. was supported by National Institute of General Medical Sciences–NIH Ruth L. Kirschstein NRSA Postdoctoral Fellowship F32GM093344. T.d. and C.B. were supported in part by National Institute of Mental Health Grant R25MH059472 while students in the Neural Systems and Behavior summer course at the Marine Biological Laboratory (Woods Hole, MA).

Correspondence should be addressed to Michael N. Nitabach, Department of Cellular and Molecular Physiology, Department of Genetics, Program for Cellular Neuroscience, Neurodegeneration and Repair, Yale School of Medicine, 333 Cedar Street, New Haven, CT 06520. E-mail: michael.nitabach@yale.edu.

DOI:10.1523/JNEUROSCI.2017-10.2011

 0270-6474/11/318181-13$15.00/0

suggest that cholinergic synaptic communication is required for lLN_v rhythmic membrane activity.

To identify the nature of synaptic inputs to lLN_vs, we used pharmacological methods to inhibit or activate a variety of neurotransmitter systems and measured the effect on lLN_v membrane activity and ionic conductances. lLN_vs receive excitatory input via nicotinic acetylcholine receptors (nAChRs) and inhibitory input via both $GABA_A$ receptors and glutamate-gated chloride channels (GluCls). Cholinergic inputs are required for lLN_v synchrony, whereas GABAergic input is not required to maintain this synchrony, but likely plays a modulatory role in lLN_v membrane activity.

Materials and Methods

Clock neuron electrophysiology

Adult Drosophila *whole-brain explant preparation.* Flies were maintained at 25°C in a 12 h light/dark (LD) cycle. *pdf-gal4;UAS-DsRedII* fly lines were used as described previously (Brand and Perrimon, 1993; Renn et al., 1999; Wu et al., 2008a). For the experiments looking at paired recordings between lLN_vs and non-LN_vs, pdf-Gal4/201Y-Gal4;UAS-dsRED flies were used and the neurons were identified by both fluorescence and anatomical position. Three to 7 d posteclosion female flies that express red fluorescent protein, DsRed, solely in ventral lateral clock neurons (LN_vs) were collected for electrophysiological recordings. Whole-cell recordings on large LN_v (lLN_vs) of fly brain explants were performed as described previously (Gu and O'Dowd, 2006; Cao and Nitabach, 2008; Wu et al., 2008a), and all individual recordings were done in light phase of LD cycle. All paired recordings were performed between zeitgeber time 22 (ZT22) and ZT23. Briefly, the fly brains were dissected in external recording solution, which consisted of the following (in mM): 101 NaCl, 3 KCl, 1 $CaCl_2$, 4 $MgCl_2$, 1.25 NaH_2PO_4, 5 glucose, 20.7 $NaHCO_3$, pH 7.2, with osmolarity of 250 mmol/kg. The brain was placed ventral side up, secured in a recording chamber with a mammalian brain slice "harp" holder, and was continuously perfused with external solution bubbled with 95% O_2/5% CO_2 at room temperature (22°C). lLN_vs were visualized by DsRed fluorescence, and subsequently, the immediate area surrounding the lLN_vs was enzymatically digested with focal application of protease XIV (2 mg/ml; Sigma-Aldrich).

Whole-cell patch-clamp electrophysiology. Whole-cell recordings were performed using borosilicate standard wall capillary glass pipettes (Sutter Instrument). Recording pipettes were filled with internal solution consisting of the following (in mM): 102 potassium gluconate, 17 NaCl, 0.085 $CaCl_2$, 4 Mg-ATP, 0.5 Na-GTP, 0.94 EGTA, and 8.5 HEPES, pH 7.2, and osmolarity of 235 mmol/kg. The resistance of filled pipettes was between 8 and 12 MΩ. Gigaohm seals were achieved before breaking in to whole-cell configuration in voltage-clamp mode, followed by break-in to whole-cell configuration while in voltage-clamp mode. To confirm maintenance of a good seal and absence of damage to the cell, a 40 mV hyperpolarizing pulse was imposed on each cell while in whole-cell voltage-clamp mode from a holding potential of −80 mV. Only if the resulting inward leak current was less than −100 pA was that cell used for subsequent current-clamp measurements of resting membrane potential (RMP), action potential (AP) firing rate, and membrane resistance. RMP was determined after stabilization of the membrane potential after the transition from voltage-clamp to current-clamp mode, and for cells with oscillating membrane potential was defined at the trough of the oscillation. AP firing rate was computed over the 5 min period after the transition from voltage-clamp to current-clamp configuration. Burst rate firing was defined as the number of bursts occurring in the last 60 s of the 5 min period after the transition from voltage-clamp to current-clamp configuration, divided by 60 s. Membrane resistance was measured by injecting −20 pA current in current-clamp recording mode. Voltage clamp was then used to record neurotransmitter-induced currents on lLN_vs held at different holding potentials in the presence of 2 μM TTX (Sigma-Aldrich), which inhibits action potential firing of neurons and communication of neural network. Glutamate-induced currents were also recorded in external solution with reduced $[Cl^-]_o$ by replacing NaCl with equal molar of Na-gluconate.

Data acquisition and analysis. Signals were measured using a Multiclamp 700B (Molecular Devices) and a Digidata 1440A (Molecular Devices).

The degree of synchrony of the pair recordings was determined by filtering 100 s of current clamp data using a low-pass Guassian filter, and then running cross-correlation analysis on the pair of recordings (Clampfit). The peak correlation value for each pair was determined. Autocorrelation was used to analyze the rhythmic RMP oscillations in 201Y+/lLN_v pairs. Again, 100 s of current-clamp data was filtered using a low-pass Guassian filter, and then autocorrelation was run (Clampfit). Pairs exhibiting strong burst firing were used for statistical analysis.

The amplitudes of neurotransmitter-induced currents were measured in Clampfit, which is part of the pClamp 10 software package. The significance tests were performed using ANOVA with Tukey–Kramer multiple comparisons on the difference of the cross-correlations of paired recordings and reversal potentials for glutamate-gated current in different $[Cl^-]_o$ solutions.

Drosophila *brain immunostaining*

Brains from pdf-Gal4/201Y-Gal4;UAS-dsRED flies were dissected, fixed with 4% paraformaldehyde, and then stained with both mouse anti-PDF (1:50) (Developmental Studies Hybridoma Bank, University of Iowa, Iowa City, IA) and rabbit anti-dsRED (1:1000) (Invitrogen) primary antibodies. PDF and dsRED were visualized using a Cy2-conjugated anti-mouse antibody (1:300) (Jackson ImmunoResearch) and a Cy3-conjugated anti-rabbit antibody (Jackson ImmunoResearch), respectively. The images were collected with a 20× objective of a Zeiss AxioExaminer Z1 microscope, using AxioVision 4 software.

Results

lLN_vs receive synchronous synaptic inputs

To address whether lLN_vs that regulate patterns of rest and arousal exhibit synchronous firing, as has been observed in neural circuits in the mushroom bodies regulating memory (Rosay et al., 2001), we performed whole-cell patch-clamp physiology on pairs of lLN_vs simultaneously (Fig. 1*A*). All paired recordings were performed at ZT22–ZT23, which was chosen to maximize the number of burst firing neurons, as the largest percentage of burst firing lLN_vs occurs at this time (Sheeba et al., 2008a). Pairs of lLN_v neurons residing in the same hemisphere exhibited synchronized rhythmic membrane activity, such that the depolarized and hyperpolarized phases occurred simultaneously. This synchrony was exhibited in all pairs from the same hemisphere that exhibited strong burst firing [peak correlation of 0.8395 ± 0.059 (SEM); $n = 8$], whereas two pairs of lLN_vs that were tonically firing did not show rhythmic membrane activity, and therefore synchrony could not be detected (Fig. 1*E*). We next recorded from pairs of lLN_vs from contralateral hemispheres (Fig. 1*B*). Interestingly, all of the pairs of bursting neurons also exhibited tight synchrony of electrical activity [peak correlation of 0.9112 ± 0.044 (SEM); $n = 5$], whereas three contralateral pairs that exhibited a mixture of tonic and burst firing showed decreased synchrony (Fig. 1*E*). The recordings that we performed suggest that each member of the pair can switch firing modes, from burst to tonic and vice versa, independently, but exhibit synchrony only in the burst firing mode. It has been suggested that this modulation between firing states may be regulated by voltage-gated calcium channels (Sheeba et al., 2008a).

To investigate whether the robust synchrony that we observed between lLN_vs represented a general synchrony of all neurons in the whole-brain preparation [analogous to epileptiform activity seen in mammalian brain slices (Fisahn, 2005) or other forms of synchronous neuronal activity] or whether it had some specificity to neurons associated with the circadian and arousal circuits, we performed paired recordings between lLN_v and a stereotyped neuron that is positive for the well studied driver 201Y-Gal4 and

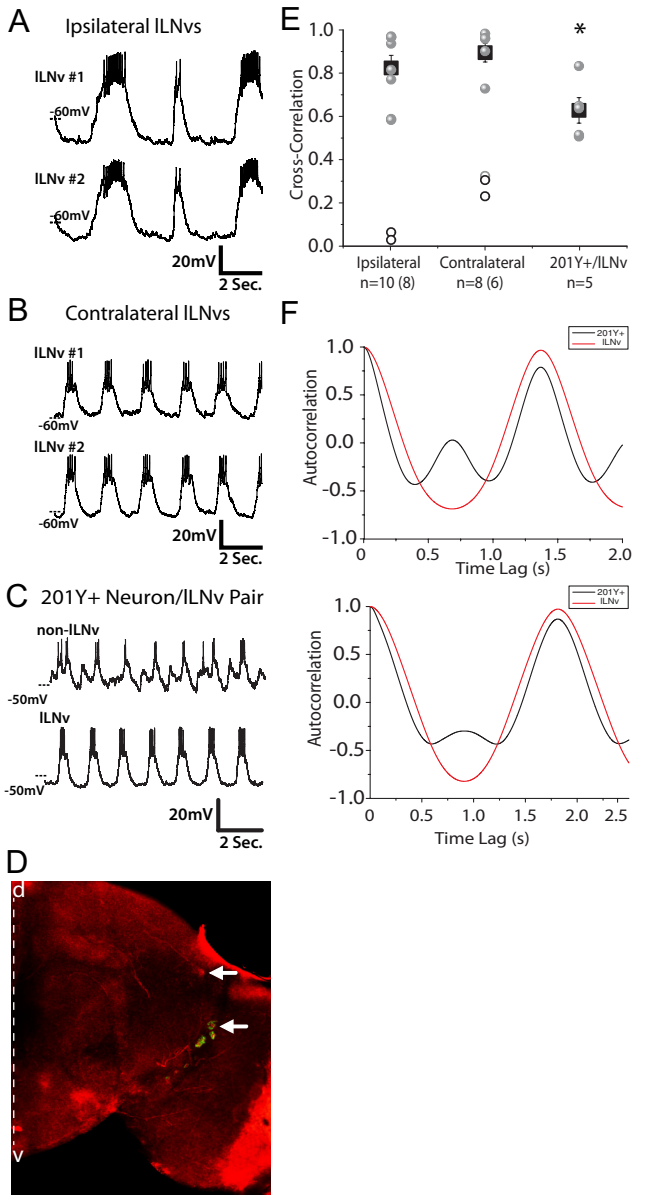

Figure 1. Bilaterally synchronous membrane activity of lLN_v rest/arousal neurons. ***A***, ***B***, Representative simultaneous whole-cell current-clamp recordings of two lLN_vs, either from ipsilateral ($n = 10$) (***A***) or contralateral ($n = 8$) (***B***) hemispheres *in situ*. ***C***, Simultaneous recording shows the partially synchronized firing patterns of one lLN_v and one 201Y+ neuron. These neurons exhibit partial synchronized membrane activity, sharing a common input, but also receiving unique input ($n = 5$). All paired recordings were performed between ZT22 and ZT23. ***D***, *Drosophila* brain at 20× magnification stained for the neuropeptide PDF in green and for dsRED (expressed using both pdf-Gal4 and 201Y-Gal4, a well characterized neuronal driver). The white arrows indicate the location and identity of the neuron pair used for 201Y+/lLN_v paired recordings. The 201Y+ neuron was PDF− and located dorsomedial to the lLN_vs. The dashed white line indicates the midline of the brain, with dorsal (d) up and ventral (v) down. ***E***, Cross-correlation analysis of paired recordings. All paired recordings, ipsilateral lLN_v, contralateral LN_v, and 201Y+/lLN_v, were filtered with a low pass Guassian filter, and then their degree of synchrony was determined by cross-correlation. The circles represent the correlational value of each pair; the gray circles indicate pairs exhibiting strong burst firing, whereas the unfilled circles represent pairs exhibiting differing degrees of tonic firing. The black squares show the mean degree of synchrony of all the bursting neurons for each condition with the error bars representing the SEM. The *n* are indicated, with the number of bursting pairs included in the mean in parentheses. The degree of synchrony of these groups were significantly different from each other (ANOVA, $p = 0.02$). An asterisk denotes statistical significance. ***F***, Autocorrelation analysis of two representative pairs of 201Y+ (black) and lLN_v (red) neurons show that they share one common synchronized peak of membrane activity but that the 201Y+ neurons exhibit a second peak of membrane activity that is not shared by the lLN_vs.

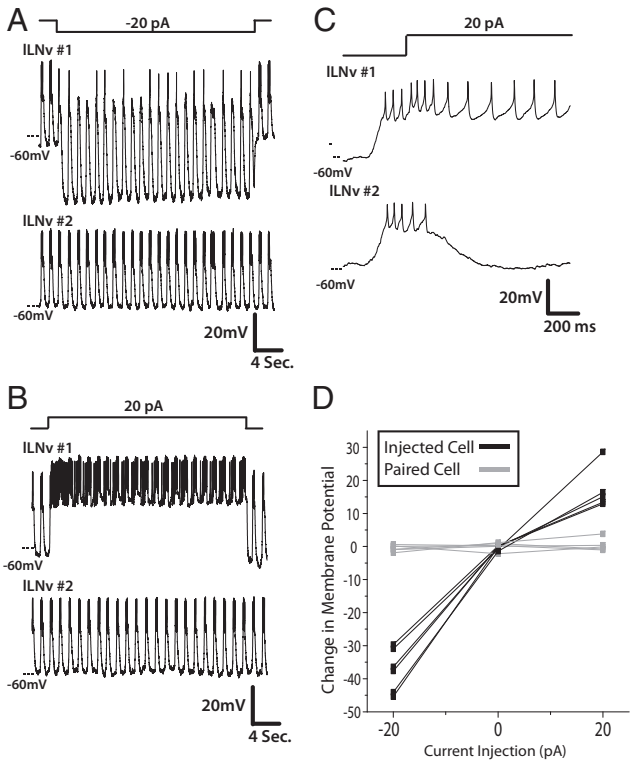

Figure 2. Synchronous membrane activity of lLN_v is attributable to synchronized synaptic input, not to coupling between the two neurons. ***A***, In this paired recording, this representative trace depicts one lLN_v that was injected with −20 pA for 30 s (top), whereas the response was simultaneously recorded in another lLN_v in the same brain hemisphere (second panel from top). In this example, the lLN_v that was injected with negative current hyperpolarized, whereas the other lLN_v was unaffected ($n = 6$). Synchrony of rhythmic membrane activity between the two lLN_vs was unaffected. All paired recordings were performed between ZT22 and ZT23. ***B***, Similarly, when 20 pA was injected for 30 s into one lLN_v (bottom), the second neuron maintains its baseline resting membrane potential and is not affected by the depolarization and action potentials induced in the first lLN_v ($n = 6$). ***C***, Zooming in on the first 1 s of the depolarizing current injection into the first lLN_v, it is clear that there is no postsynaptic response of the second lLN_v to the action potential firing in the first. ***D***, Quantification of the effect of current injection on both neurons during paired recordings, described above ($n = 6$). The injected neurons (black) exhibit clear changes in membrane potential as a result of being injected with either positive or negative current, whereas each paired neuron that is concurrently recorded but not injected (gray) does not show any change in membrane potential.

is located dorsal to the lLN_vs ($n = 5$) (Fig. 1*C*,*D*). All 201Y+/lLN_v pairs exhibited one peak of synchronized membrane activity, but the 201Y+ neurons all demonstrated an additional peak of rhythmic membrane activity of a different phase, not seen in the lLN_vs (Fig. 1*C*,*F*). In addition, the degree of synchrony that we see between these pairs of 201Y+ and lLN_v neurons is significantly different from the robust synchrony seen in contralateral lLN_v–lLN_v pairs (ANOVA, $p = 0.02$, $p < 0.05$) (Fig. 1*E*). These data show that, whereas both lLN_vs and the 201Y+ neurons receive some common rhythmic inputs, the 201Y+ neurons also receive unique inputs and are less synchronized with lLN_vs than lLN_vs are to each other.

To determine whether this highly synchronized electrical activity between pairs of lLN_v neurons is a result of synchronized synaptic inputs or, rather, because of direct communication between lLN_vs, we examined the effect of silencing or exciting one member of a pair on the membrane activity of the other. To do this, we achieved paired recordings from two lLN_vs from ipsilateral ($n = 5$) or contralateral ($n = 4$) hemispheres, then injected negative or positive current into one of the pair to induced either

silencing or activation, respectively, and observed the pattern of firing in the other member of the pair. Injection of negative current into lLN_v 1 hyperpolarized the neuron and suppressed much of its action potential firing; the membrane potential of this neuron continued to oscillate around this hyperpolarized baseline (Fig. 2*A*, top trace), indicating that this neuron was still receiving rhythmic synaptic inputs. When we simultaneously observed the electrical activity of lLN_v 2, it exhibited unchanged membrane activity, continuing to fire action potentials, in the same way as before the current injection into its counterpart (Fig. 2*A*, second trace from top). These two lLN_vs still exhibited synchronized rhythmic membrane activity. We observed no effect on the membrane activity of one lLN_v by injecting negative current into another in all pairs examined ($n = 9$; 5 ipsilateral pairs, 4 contralateral pairs). Similarly, when one lLN_v was injected with positive current, the neuron was triggered to fire a burst of action potentials, whereas its pair stayed at a resting phase before both neurons receive synchronized synaptic inputs (Fig. 2*B*). Despite this positive current injection into lLN_v 1, lLN_v 2 continued to receive synaptic input, as evidenced by its exhibiting postsynaptic potentials (PSPs). This input was not from its paired lLN_v since the action potentials fired in lLN_v 1 did not correspond to the PSPs seen in lLN_v 2 (Fig. 2*C*). We observed similar results with all pairs injected with positive current ($n = 9$; 5 ipsilateral pairs, 4 contralateral pairs). In all cases, current injection into one lLN_v caused a change in membrane potential in that neuron, but not in the lLN_v that was simultaneously being recorded from (Fig. 2*D*). This suggests that lLN_vs receive synchronous synaptic inputs from neuron populations distinct from the lLN_vs themselves. An additional possibility is that silencing one lLN_v in the context of the network of eight lLN_vs is not sufficient perturbation to disrupt the rhythmic membrane activity of another lLN_v, even if these neurons are synaptically connected. We do not believe this is the case, however, since severing the posterior optic tract, a manipulation that blocks communication from all lLN_vs in the contralateral hemisphere, had no effect on synchronous membrane activity of contralateral pairs of lLN_vs (data not shown).

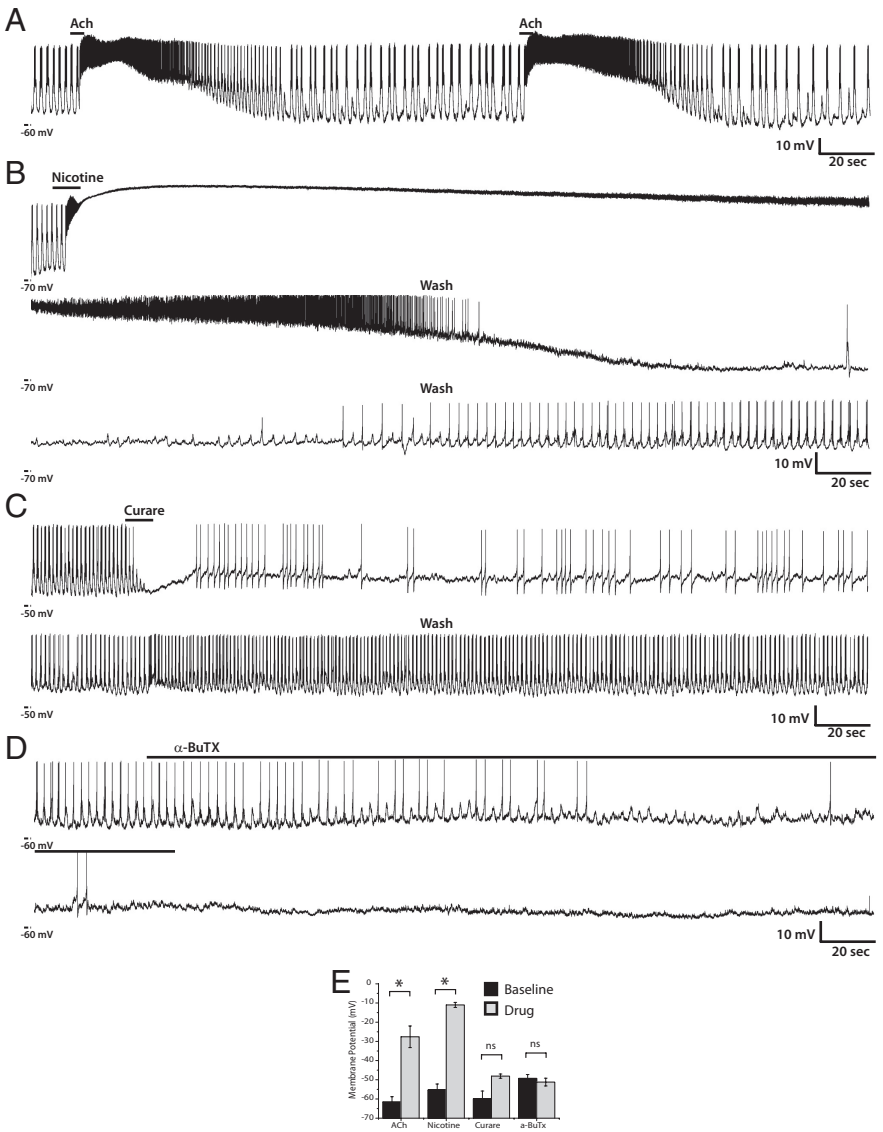

Figure 3. Modulation of lLN_v membrane activity by nAChR agonists and antagonists. ***A–D***, Representative whole-cell current-clamp recordings of single lLN_vs *in situ*. ***A***, This recording shows one example of an lLN_v treated two times consecutively with 1 mM ACh for 5 s. ACh increased membrane activity of the lLN_v, depolarizing membrane potential and increasing firing rate. This effect was reversible and replicable ($n = 4$). ***B***, One example of lLN_v current-clamp recording showing the effect of the nAChR agonist nicotine. The lLN_v was exposed to 2 mM nicotine for 10 s. Membrane potential and action potential firing rate were dramatically increased ($n = 8$). After the end of nicotine exposure, the RMP and AP firing rate decreases slowly and the neuron exhibits a refractory phase. The bottom and middle panels show the rest of the washout of the drug, which was only partially reversible in seven of eight neurons. ***C***, ***D***, These are representative recordings of lLN_vs treated with nAChR antagonists curare (200 μM) ($n = 6$) (***C***) or α-bungarotoxin (0.5 μM) (***D***). The inhibitory effects of curare are reversible, whereas the effects of α-bungarotoxin were irreversible, not reversing after >30 min of washout (data not shown). ***E***, Quantification of changes in membrane potential because of drug treatment. The black bars indicate the mean resting membrane potential of the neurons before drug treatment, whereas the gray bars show the RMP of the cell after pharmacological manipulation. The error bars represent the SEM. Both ACh and nicotine induced significant changes in RMP ($p = 0.0016$ and $p = 0.0007$, respectively), whereas curare and α-bungarotoxin did not. $N > 5$ for each treatment. *, Statistically significant difference; ns, not significant.

Nicotinic acetylcholine receptors mediate excitatory inputs to lLN_vs

Since acetylcholine is the most prevalent excitatory fast synaptic neurotransmitter in the insect CNS (Bossy et al., 1988; Schuster et al., 1993; Yasuyama and Salvaterra, 1999; Littleton and Ganetzky, 2000), we reasoned that cholinergic input was likely a major influence on lLN_v membrane activity. To test this hypothesis, we examined the participation of cholinergic signals in lLN_v membrane activity by performing whole-cell patch-clamp recordings on single lLN_vs in current-clamp mode, with bath application of agonists or antagonists of acetylcholine receptors. The representative lLN_v in Figure 3*A* exhibits oscillations in RMP between −55 and −40 mV with a burst of six to eight action potentials during the depolarized phase. When the preparation was bath-

treated with 1 mM acetylcholine (ACh), the membrane dramatically depolarized and experienced a burst of APs, lasting tens of seconds (Fig. 3*A*,*E*). After returning to normal saline bath, the membrane gradually repolarized and membrane activity returned to baseline. This effect on membrane potential was repeatable and significant not only in this same neuron, but also in other lLN_vs in independent whole-brain explants ($p = 0.004$; $n = 4$).

Two different types of ACh receptors have been identified in the *Drosophila* nervous system, ionotropic and metabotropic (Bossy et al., 1988; Schuster et al., 1991; Blake et al., 1993). To specifically test the effect of ionotropic ACh receptors on membrane activity of lLN_vs, we bath-applied a specific ionotropic agonist, nicotine, and recorded the resulting response in current-clamp mode. When 2 μM nicotine was added to the external solution, lLN_vs underwent dramatic depolarization of their membrane potential, which, after a small amount of repolarization, was followed by a burst of AP firing and then a plateau (Fig. 3*B*,*E*). The depolarized plateau ranged from -20 to -6 mV (mean, -10.97 ± 1.31 mV) with a duration of 14 to 200 s ($n = 8$), continuing long after the removal of nicotine from the bath solution. The membrane potential during nicotine treatment significantly elevated over baseline ($p < 0.00001$). The prolonged nature of this effect could possibly be attributable to the very high affinity for this agonist to its receptor. The depolarized state gradually gave way to repolarization of the RMP and a decrease in AP firing. Interestingly, these neurons exhibited a refractory phase before returning to rhythmic AP firing. This effect was only partially reversible, as only one neuron of eight tested returned back to its firing rate before nicotine application. This complex response of lLN_vs to nicotine raises the possibility that this nAChR agonist not only excites lLN_v membrane activity but also excites inhibitory synaptic inputs to lLN_vs, as suggested by the refractory phase after repolarization. To test the effect of metabotropic ACh receptors on lLN_v membrane activity, muscarine, a metabotropic AChR agonist, was applied to the external solution and the response was recorded (supplemental Fig. 1, available at www.jneurosci.org as supplemental material). This treatment induced no significant depolarization or change in interval between bursts of APs but did result in an increase in AP number (mean baseline AP firing rate, 1.925 ± 0.248 Hz; mean muscarine AP firing rate, 4.1 ± 0.414 Hz; $p < 0.004$), which was a less dramatic response compared with that elicited by the ionotropic agonist, nicotine.

Given that the nicotinic agonist induced such a strong response from lLN_vs, we examined the effect of nAChR antagonists, curare and α-bungarotoxin (α-BuTX) on lLN_v membrane activity. Bath application of 200 μM curare eliminated AP firing almost immediately, but did not change membrane potential, and was completely reversible on washout of the drug in four of six neurons tested (one neuron showed only partial recovery) (Fig. 3*C*,*E*). Similarly, α-BuTX inhibited membrane activity of lLN_vs, but did not change membrane potential ($n = 14$) (Fig. 3*D*,*E*), although the kinetics of its effect were slower than that of curare, possibly because of the fact that curare is a small molecule, as opposed to a peptide like α-BuTX, and therefore was able to diffuse into (and out of) the whole-brain preparation more quickly. In the representative trace shown in Figure 3*D*, on addition of 0.5 μM α-BuTX, the lLN_v exhibited progressively decreased firing with an ~5 mV oscillation in RMP, which transitioned to complete abolition of AP firing and a relatively stable RMP (Fig. 3*D*). Of the 14 neurons tested, α-BuTX caused complete cessation of AP firing in 10 lLN_vs and partial block of AP firing in the other four. The inhibitory effect of this toxin was not reversible, as washout led to only partial recovery in eight neurons and no detectable recovery in six. Importantly, curare or α-BuTX blockade of nAChR each resulted in loss of rhythmic oscillation in membrane potential, indicating that these oscillations are not intrinsic pacemaker potentials, but rather are imposed by synchronized synaptic inputs.

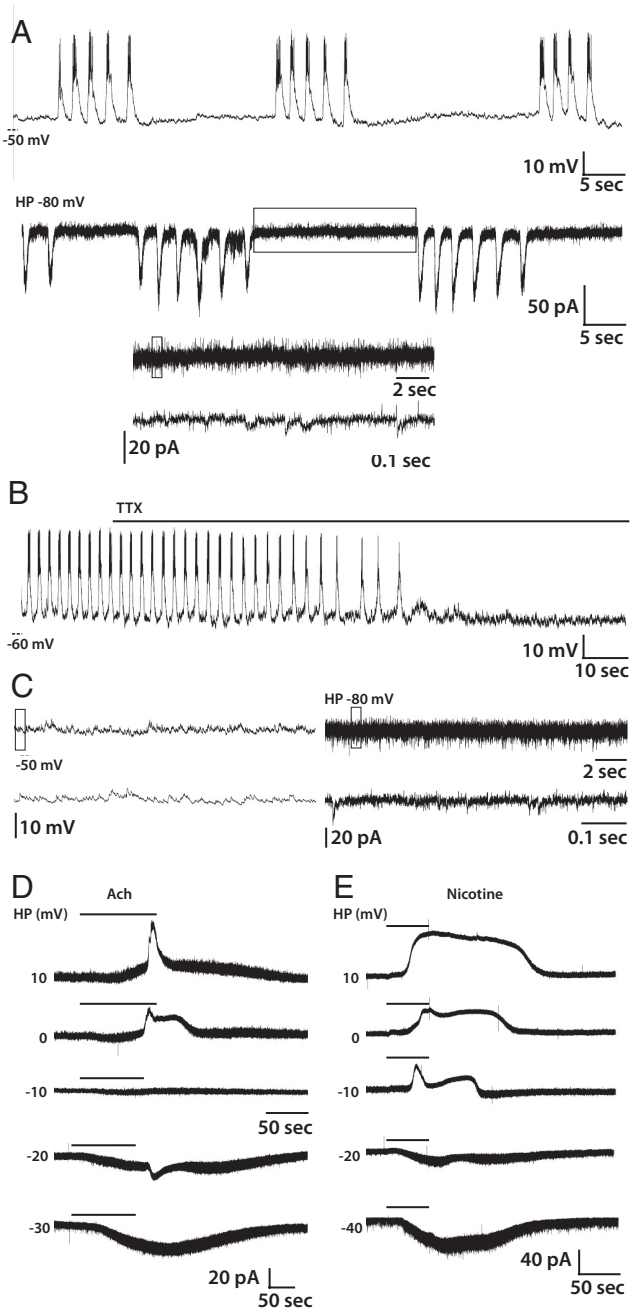

Figure 4. nAChR currents of lLN_vs. ***A***, Representative trace of lLN_v spontaneous activity in current-clamp mode (***A***, top) or voltage-clamp mode with a holding potential of -80 mV (***A***, middle). The bottom two traces in ***A*** are enlargements of parts of the rest phase that are boxed in the panel directly above each one. ***B***, Representative current-clamp recording of lLN_v treated with TTX. TTX abolished action potentials and rhythmic membrane activity. ***C***, Representative current-clamp (left) and voltage-clamp (right) recordings from a single lLN_v treated with TTX and magnified views of the regions boxed in each top panel, respectively. Miniature postsynaptic potentials (left) and currents (right) are visible. ***D***, ***E***, Voltage-clamp recordings of ACh- (***D***) or nicotine-induced (***E***) currents in individual lLN_vs at a range of holding potentials (10, 0, -10, -20, or -30 mV). ACh- and nicotine-induced currents reversed around -10 mV.

The inhibition of action potential firing in lLN_vs by curare and α-BuTX and dramatic depolarization induced by nicotine sug-

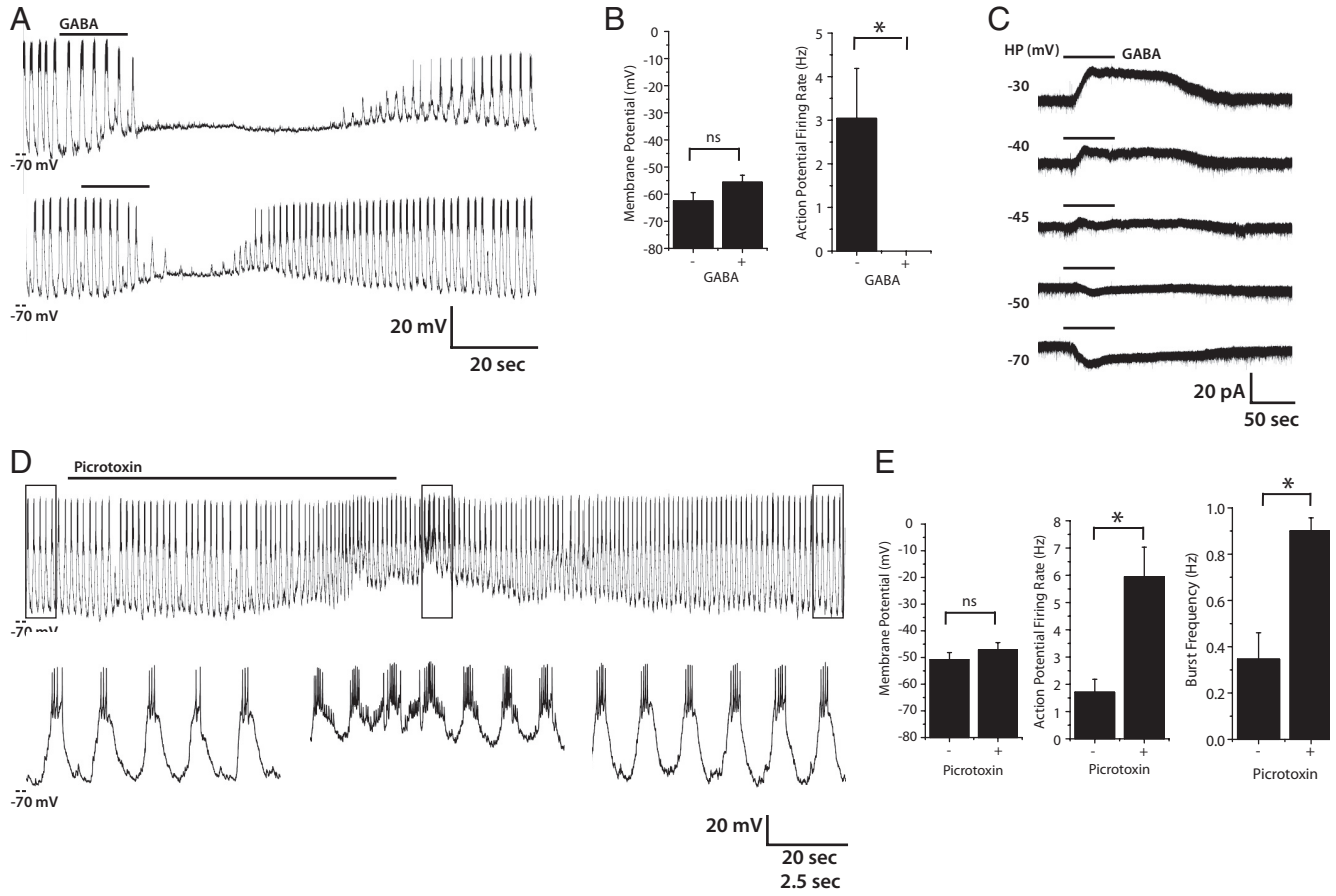

Figure 5. GABAergic modulation of lLN_v membrane activity. ***A***, Representative current-clamp recording of lLN_v responses to bath-applied GABA (1 mM) ($n = 5$). In two trials on the same lLN_v, GABA reversibly abolished action potentials and rhythmic membrane activity. ***B***, Quantification of the effect of GABA on RMP and action potential firing of lLN_vs. The black bars represent the mean RMP (left) or action potential firing rate (right), before and after GABA treatment. The errors bars equal the SEM. Treatment of lLN_vs with GABA causes a significant decrease in AP firing ($p = 0.029$) while causing no change in RMP ($p > 0.05$). *, Statistically significant difference; ns, not significant. ***C***, Voltage-clamp measurement of GABA (1 mM)-induced currents at a range of holding potentials (−30, −40, −45, −50, or −70 mV) in the presence of TTX. GABA-induced currents reversed between −45 and −50 mV, near the calculated equilibrium potential of Cl^-. ***D***, Representative current-clamp recording of lLN_v treated with the chloride channel antagonist picrotoxin (100 μM) ($n = 9$). Picrotoxin causes the trough of rhythmic membrane activity to be more depolarized and increases the number of action potentials in each burst (top). Bottom traces are enlargements of boxed regions in the top trace. ***E***, Quantification of the effect of picrotoxin on RMP, action potential firing, and burst firing frequency of lLN_vs. The black bars represent the mean RMP (left), action potential firing rate (middle), or burst firing frequency (right) before and after picrotoxin treatment. The errors bars equal the SEM. Treatment of lLN_vs with picrotoxin causes a significant increase in AP firing ($p = 0.0025$) and in burst firing frequency ($p = 0.0008$) while causing no significant change in RMP ($p > 0.05$). *, Statistically significant difference; ns, not significant.

gest that nAChRs mediate excitatory synaptic input to these neurons. However, this does not rule out the possibility that the observed effects are not attributable to direct cholinergic synaptic input into lLN_vs, but rather indirect effects from intermediary neurons interposed between cholinergic neurons and lLN_vs. To directly assess nAChR-mediated currents in lLN_vs, we used voltage clamp to measure ACh-induced currents in the presence of bath-applied TTX. TTX blocks voltage-gated sodium channels in all neurons in the whole-brain explant, thus inhibiting AP firing in all neurons and thereby preventing all nonspontaneous synaptic activity. In normal bath solution, lLN_vs exhibit spontaneous action potential firing, tonic or bursting, and often oscillations in RMP (Fig. 4*A*, top trace). In voltage-clamp mode with a holding potential of −80 mV, lLN_vs exhibit rhythmic large inward currents of ~100 pA, corresponding to AP-dependent excitatory synaptic inputs, and also showed small inward currents, ranging in amplitude from 2 to 10 pA, during the resting phase (Fig. 4*B*, bottom traces). When TTX was added to the bath solution, action potential firing and rhythmic membrane activity were blocked (Fig. 4*B*). However, small TTX-resistant transient depolarizations could still be observed in current clamp (Fig. 4*C*, left traces) and corresponding inward currents in voltage clamp (Fig. 4*C*, right traces). It is reasonable to conclude that the TTX-resistant small inward currents are miniature postsynaptic currents (mPSCs), mediated by spontaneous vesicle release by presynaptic neurons with input into lLN_vs. The amplitude of these miniature currents is similar to those observed in Kenyon cells in the *Drosophila* mushroom body (Su and O'Dowd, 2003). The effect of TTX on lLN_v that we observe is consistent with the effect of TTX on lLN_vs previously reported (Sheeba et al., 2008a), despite the fact that they used a 20-fold lower dose.

In our experimental paradigm, we first established a robust recording, assessing the membrane activity of a lLN_v in current-clamp mode, and then added TTX and monitored the loss of APs, as in Figure 4*B*. We then recorded AChR agonist-induced currents at a series of holding potentials and determined the reversal potential for these currents by assuming a linear relationship in this range of holding potentials for each individual neuron. In the representative recording in Figure 4*D*, application of 1 mM ACh induced an outward current at potentials positive to −10 mV and an inward current at potentials negative to −20 mV (Fig. 4*D*). After the reversal potential was determined for multiple individual lLN_vs ($n = 7$), the reversal potential of the current was determined by averaging the reversal potentials of each individual

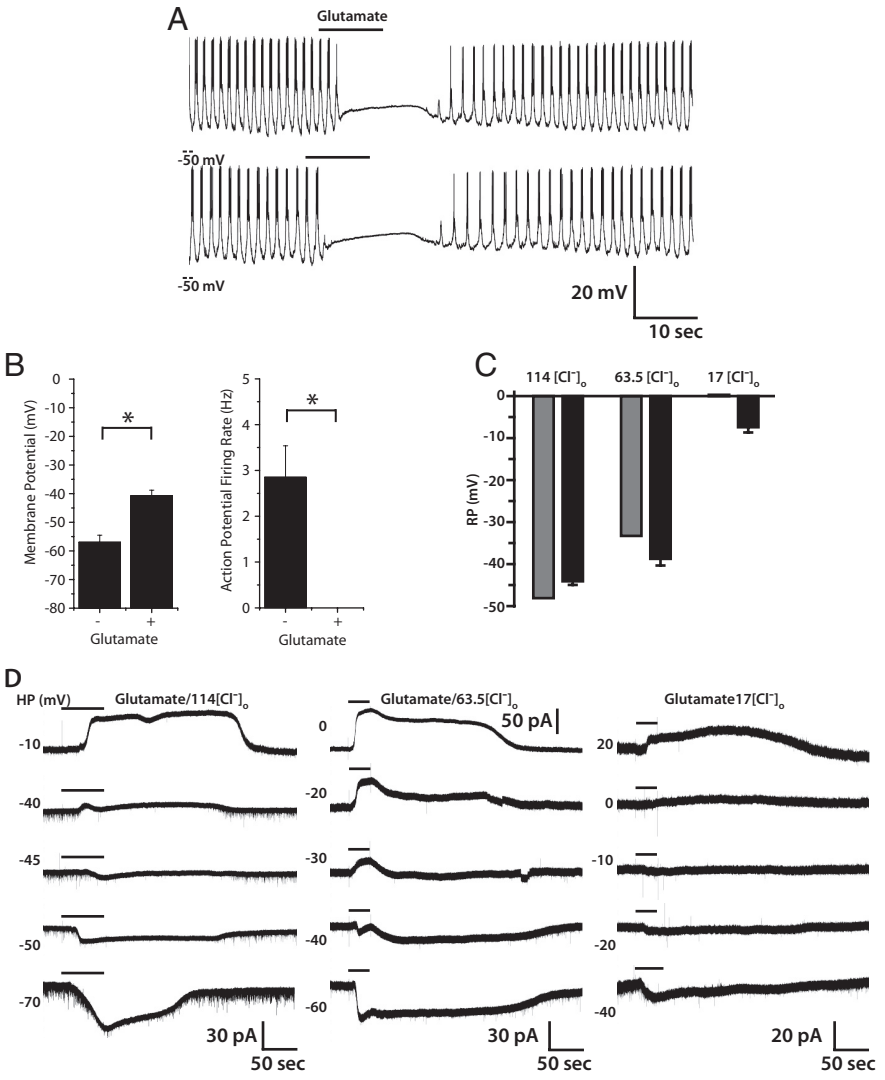

Figure 6. Glutamatergic modulation of lLN_v membrane activity. Representative current-clamp recording of lLN_v responses to bath-applied glutamate (1 mM). ***A***, In two trials on the same lLN_v, glutamate (1 mM) reversibly abolished action potentials and rhythmic membrane activity ($n = 5$). ***B***, Quantification of the effect of glutamate on RMP and action potential firing of lLN_vs. The black bars represent the mean RMP (left) or action potential firing rate (right), before and after glutamate treatment. The errors bars equal the SEM. Treatment of lLN_vs with glutamate causes a significant increase in RMP ($p = 0.0008$) and a concurrent decrease in AP firing ($p = 0.003$). *, Statistically significant difference; ns, not significant. ***C***, Voltage-clamp measurement of glutamate (1 mM)-induced currents in the presence of TTX. Glutamate-induced currents reversed at holding potentials that varied with $[Cl^-]_o$ and were near the calculated reversal potentials Cl^- at each $[Cl^-]_o$. ***D***, Quantification of the experimentally observed reversal potentials of glutamate-induced currents at different $[Cl^-]_o$ (black bars) versus the calculated reversal potential. The error bars depict the SEM.

neuron (supplemental Fig. 2, available at www.jneurosci.org as supplemental material). The reversal potential for the ACh-induced current was -8.9 ± 1.4 mV (SEM). Similarly, we recorded nicotine-induced currents in lLN_vs (representative trace) (Fig. 4*E*) and subsequently determined the reversal potential for the nicotine-induced current to be -14.9 ± 1.4 mV (supplemental Fig. 2, available at www.jneurosci.org as supplemental material). As expected, the experimentally measured reversal potentials for ACh- and nicotine-induced currents are near the predicted reversal potential for a nonselective monovalent cation channel. These data confirm that nAChRs are present in lLN_vs and mediate excitatory synaptic input.

Both the ACh- and nicotine-induced currents displayed a slightly delayed onset in relation to the bath application of the agonist and also exhibited repeatable complex time courses of activation. These repeatable time courses could be attributable to a variety of factors, including kinetics of wash-in of the agonist to various regions of the extensive dendritic arbors of the lLN_vs, on and off binding kinetics of agonist with the receptor, desensitization of the receptors, or the inability to hold the whole surface of the neuron at the holding potential set at the soma.

$GABA_A$ receptors mediate inhibitory synaptic inputs to lLN_vs

GABA is a major inhibitory neurotransmitter in insects and is widely distributed in the CNS (ffrench-Constant et al., 1991; Aronstein and ffrench-Constant, 1995; Hosie et al., 1997; Littleton and Ganetzky, 2000). Since lLN_vs have been shown to express the $GABA_A$ receptor and since flies with decreased $GABA_A$ receptor expression in their LN_vs show disrupted rest (Parisky et al., 2008; Chung et al., 2009), we hypothesized that GABA might be an important inhibitory input into lLN_vs. To test this, we first examined the effect of GABA application on the membrane activity of lLN_vs in current-clamp mode. When GABA (1 mM) was added to the external solution, AP firing was rapidly blocked ($n = 5$), but the membrane potential was not significantly altered ($p > 0.05$). This effect was reversible and could be repeated in the same neuron (Fig. 5*A*,*B*). This activation of GABA receptors also resulted in a loss of oscillations in resting membrane potential in lLN_vs. Conversely, when picrotoxin, a $GABA_A$ receptor antagonist, was bath applied, it increased firing rate (mean baseline AP firing, 1.7 ± 0.474 Hz; mean picrotoxin AP firing rate, 5.94 ± 1.09 Hz; $p = 0.0025$) and also increased the frequency of firing bursts (mean baseline burst frequency, 0.346 ± 0.114 Hz; mean picrotoxin burst frequency, 0.9 ± 0.057; $p = 0.0008$). The picrotoxin effect was also reversible.

To determine whether this response could result from GABA-induced currents within lLN_vs themselves, we performed voltage-clamp recordings in the presence of TTX (as in Fig. 4 above). Application of GABA induced an outward current at holding potentials at -45 mV or above and an inward current at potentials of -50 mV or below (Fig. 5*C*). We determined the reversal potential of the GABA-induced current in lLN_vs to be -48 ± 0.6 mV ($n = 5$) (supplemental Fig. 2, available at www.jneurosci.org as supplemental material), which is near the calculated equilibrium potential for Cl^-, -48.1 mV. These results strongly suggest that the $GABA_A$ receptor is present in lLN_vs and that these receptors mediate fast inhibitory synaptic inputs, which are important for appropriate regulation of rest and arousal (Parisky et al., 2008; Chung et al., 2009). These data are consistent with previous physiological recordings demonstrating $GABA_A$-mediated currents in dissociated PDF-positive neurons in culture (Chung et al., 2009).

Glutamate-gated Cl^- channels mediate inhibitory input to lLN_vs

Glutamate is an important inhibitory neurotransmitter in invertebrate nervous systems, as it gates the GluCl that is not present in mammals or other vertebrates (Cully et al., 1994, 1996; Dent et al., 1997, 2000; Laughton et al., 1997; Vassilatis et al., 1997; Cook et al., 2006). GluCl critically regulates patterns of locomotor activity and pharynx function in *Caenorhabditis elegans* (Dent et al., 1997; Cook et al., 2006). Although this neurotransmitter receptor was cloned in *Drosophila* by homology with its *C. elegans* counterpart (Cully et al., 1994) and its physiology has been characterized *in vitro* (Cully et al., 1996), we are unaware of any functional role for GluCl that has been identified in *Drosophila in vivo*. To test the hypothesis that GluCl inhibits network activity, we recorded from lLN_vs in current-clamp mode and applied 1 mM glutamate in the bath. As predicted by GluCl biophysical properties, glutamate application immediately blocked AP firing, and stabilized membrane potential at around −40 mV, which was reversed on washout (Fig. 6*A*) ($n = 5$). The mean baseline resting membrane potential before addition of glutamate was -57.0 ± 2.43 mV, but depolarized to -40.8 ± 1.97 mV after glutamate treatment ($p = 0.0008$) (Fig. 6*B*).

To determine whether this effect of glutamate on lLN_v membrane activity could be mediated by direct activation of GluCl channels in lLN_vs themselves, we performed voltage-clamp recordings in the presence of bath-applied TTX to record glutamate-induced currents of lLN_vs. Glutamate induces an inward current at holding potentials of −45 mV or below and an outward current at −40 mV or above, as shown in a representative cell in Figure 6*C*. After repeating this in multiple lLN_vs ($n = 8$), we determined the reversal potential to be -44.1 ± 0.6 mV (supplemental Fig. 2, available at www.jneurosci.org as supplemental material), which, similar to the GABA-induced current (Fig. 5), is close to the equilibrium potential of Cl^-. To confirm that the ionic basis for the glutamate-induced current in lLN_vs is Cl^-, we recorded the glutamate-induced current in external solutions with reduced $[Cl^-]_o$. When we reduced $[Cl^-]_o$, the reversal potential of the current became significantly more depolarized ($p < 0.001$, ANOVA) (Fig. 6*D*; supplemental Fig. 2, available at www.jneurosci.org as supplemental material), and closely tracked the predicted Cl^- equilibrium potentials. Together, these data indicate that Cl^- is the primary ionic basis for the glutamate-induced current and that GluCl channels in lLN_vs contribute to their synaptic inhibition. One alternative possibility, however, is that the effect of glutamate on lLN_v firing rate is not attributable to GluCl conductance, but rather attributable to activation of metabotropic glutamate receptors, whose downstream G-protein-dependent signaling causes the opening of a chloride ion channel, resulting in a current that reverses at the chloride reversal potential. Although this is a formal possibility, we consider it more likely that GluCl is responsible for the current we observe, as the role of mGluR on ionic conductance has been widely investigated in the literature and no such activation of chloride channels by mGluR signaling has been observed.

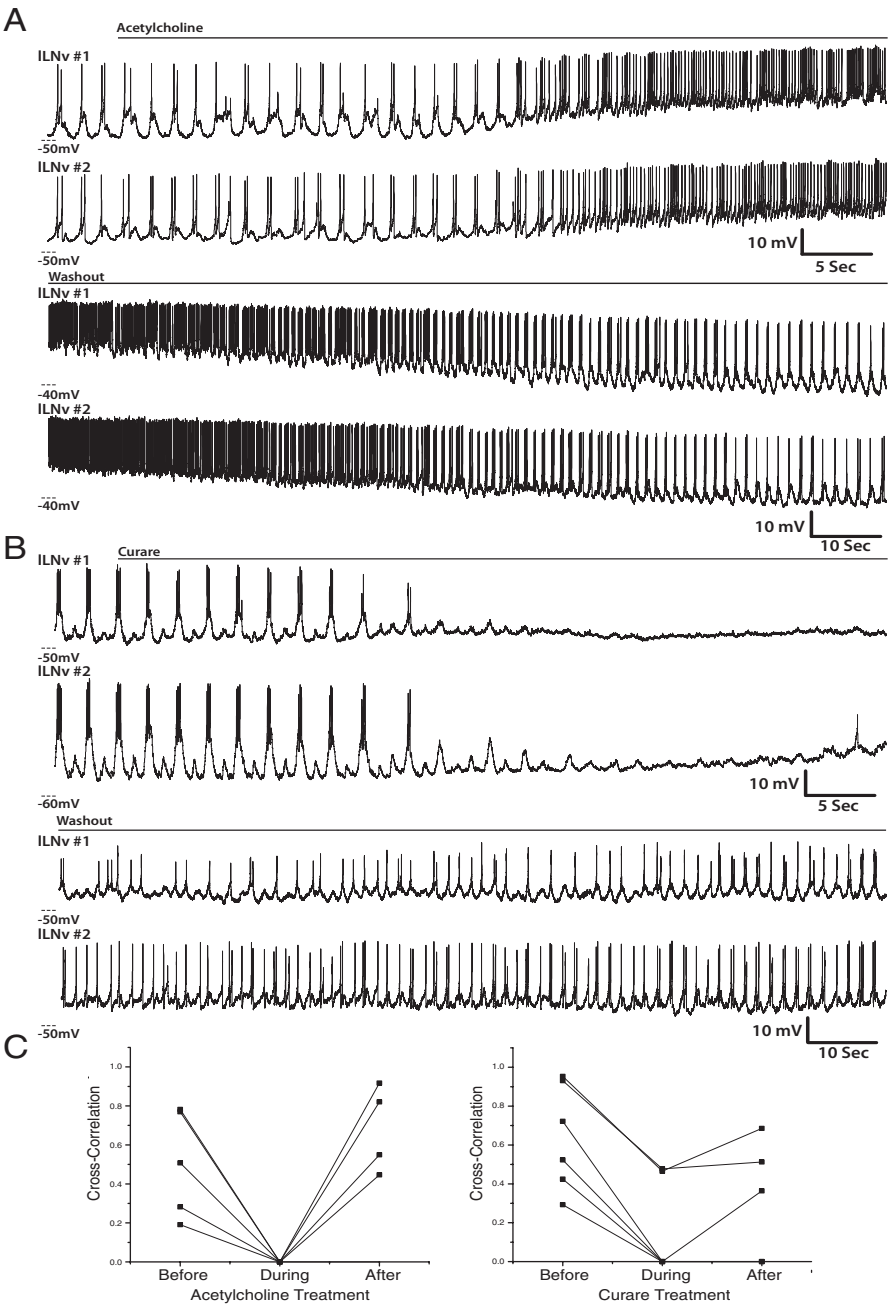

Figure 7. Activation of ACh receptors or inhibition of cholinergic inputs disrupts lLN_v synchrony. ***A***, Representative simultaneous whole-cell current-clamp recordings of two ipsilateral lLN_vs treated with ACh (1 mM) ($n = 5$), which was then washed out (bottom traces). All paired recordings were performed between ZT22 and ZT23. ***B***, Representative simultaneous whole-cell current-clamp recordings of two ipsilateral lLN_vs treated with curare (200 μM) ($n = 6$), which was then washed out (bottom traces). ***C***, Quantification of the correlation of membrane activity between pairs of lLN_vs before, during, and after ACh (left) or curare (right) treatment. Each pair that was treated with these agents is shown ($n = 5$ and $n = 6$, respectively).

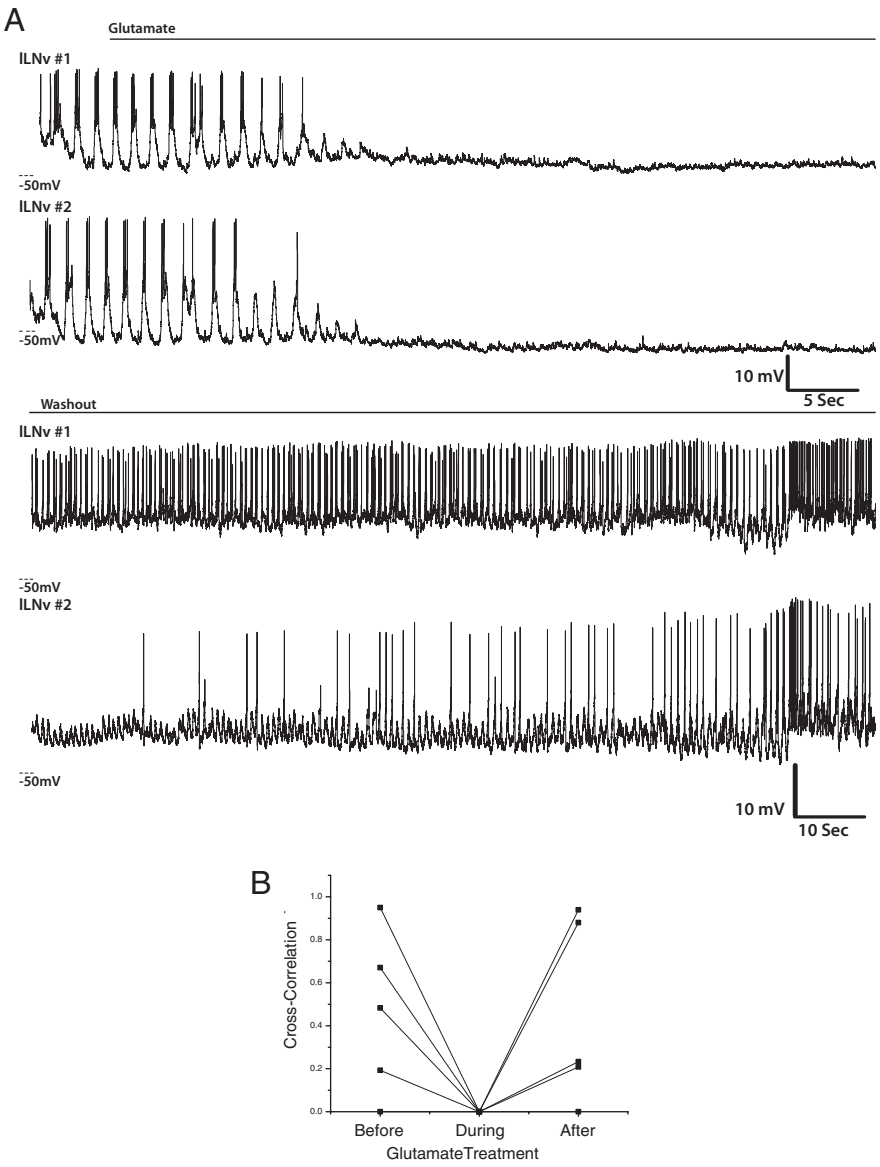

Figure 8. Activation of glutamate receptors silences synchronous lLN_v firing. ***A***, Representative simultaneous whole-cell current-clamp recordings of two ipsilateral lLN_vs treated with glutamate (1 mM) ($n = 5$), which was then washed out (bottom traces). All paired recordings were performed between ZT22 and ZT23. ***B***, Quantification of the correlation of membrane activity between pairs of lLN_vs before, during, and glutamate treatment. Each pair that was treated with these agents is shown ($n = 5$).

Cholinergic inputs, but not GABAergic inputs, are required for lLN_v synchrony

Our data suggest that lLN_vs receive cholinergic, GABAergic, and glutamatergic inputs, so we next investigated the neurochemical basis for the robust synchronous synaptic inputs that we observed in pairs of lLN_v neurons. To do this, we performed whole-cell patch-clamp physiology on ipsilateral pairs of lLN_vs simultaneously, then applied either ACh, curare, glutamate, or picrotoxin to the bath and observed the response of both neurons. All pairs of lLN_vs treated with ACh or curare, to activate or inhibit cholinergic synaptic input, showed a dramatic decrease in synchrony during treatment (Fig. 7) ($n = 5$ and $n = 6$, respectively). On washout, 6 of 11 pairs regained synchronous membrane activity (Fig. 7*C*). Of the pairs that regained synchrony on washout, four regained burst firing simultaneously. In the case of the other two pairs, one cell regained burst firing first, whereas the other fired tonically, but regained burst firing later in the washout.

Similarly, when lLN_vs were treated with glutamate, all synchronous membrane activity between lLN_v pairs was lost (Fig. 8) ($n = 5$). In several cases, synchronized burst firing returned on washout (four of five pairs), but as with cholinergic agent washout, the timing of the return to synchrony was variable, with two pairs beginning burst firing simultaneously and two regaining rhythmic membrane activity independently.

In contrast, treatment of these neurons with picrotoxin, which inhibited endogenous GABAergic input to these neurons, did not lead to loss of synchrony between the two neurons (Fig. 9*A*,*B*) ($n = 5$). In fact, two pairs of neurons that were tonically firing, and therefore not exhibiting synchronous firing before picrotoxin treatment, began burst firing and became more synchronized with picrotoxin treatment (Fig. 9*C*). These data are a stark contrast to the effect we observed when we inhibited endogenous cholinergic signaling with curare. In the case of curare, inhibition of the endogenous cholinergic input lead to complete abolition of synchronous membrane activity between lLN_v pairs. Because of the lack of a specific GluCl antagonist, we could not directly test the necessity of endogenous glutamatergic input in lLN_v synchrony. Together, these data suggest that endogenous cholinergic input is essential for lLN_v synchronous membrane activity, whereas GABAergic input is not required, but can modulate the firing properties of the neurons.

Discussion

Through the use of simultaneous dual whole-cell patch-clamp recordings in *Drosophila* whole-brain explants, we observed synchronous membrane activity in lLN_vs mediated by bilateral synaptic inputs. Pairs of lLN_vs from either the same or contralateral hemispheres exhibited synchronous rhythms of membrane activity (Fig. 1*A*,*B*). Our data indicate that this robust synchrony is attributable to synchronized network synaptic inputs, as opposed to direct electrical or synaptic coupling between lLN_vs, as manipulation of the membrane activity of one neuron through negative or positive current injection did not alter the membrane activity of its synchronous pair (Fig. 2).

It has been previously shown that neural circuits responsible for generating circadian rhythms and also those neural networks controlling rest and arousal exhibit synchronous membrane activity both in mammals and in insects (Nitz et al., 2002; Schneider and Stengl, 2005; Welsh et al., 2010). Furthermore, it has been shown that neuropeptides, VIP and PDF, in mammals and flies, respectively, and the classical neurotransmitter, GABA, play critical roles in this synchrony (Inouye and Kawamura, 1979; Welsh et al., 1995; Wagner et al., 1997; Liu and Reppert, 2000; Shirakawa et al., 2000; Albus et al., 2005; Aton et al., 2005, 2006; Schneider

and Stengl, 2005). Furthermore, we found that stereotyped neurons that were positive for a well studied driver exhibited varying degrees of synchrony with lLN_v membrane activity (Fig. 1*C*,*E*). This is consistent with a model in which certain neurons receive some of the same inputs as lLN_vs and some unique inputs. Similar to our observations in *Drosophila*, neurons in some mammalian brain regions outside the suprachiasmatic nucleus (SCN) exhibit synchronized membrane activities with SCN neurons (Inouye and Kawamura, 1979). Our data do not, however, preclude the possibility that the synchrony that we observe is attributable to widespread epileptiform or other widespread synchronous brain activity that is not specific to lLN_vs. We do not favor this explanation because we have observed lLN_v pairs exhibiting varying degrees of synchrony and also lLN_v pairs in which one cell is burst firing while the other is tonically firing, as shown in our paired recording pharmacology experiments. Even if it is the case that the synchronized activity that we see is attributable to some sort of epileptiform or other widespread synchronous activity, the nature of and mechanisms underlying this activity are still informative, as it provides insight into the connectivity of the network.

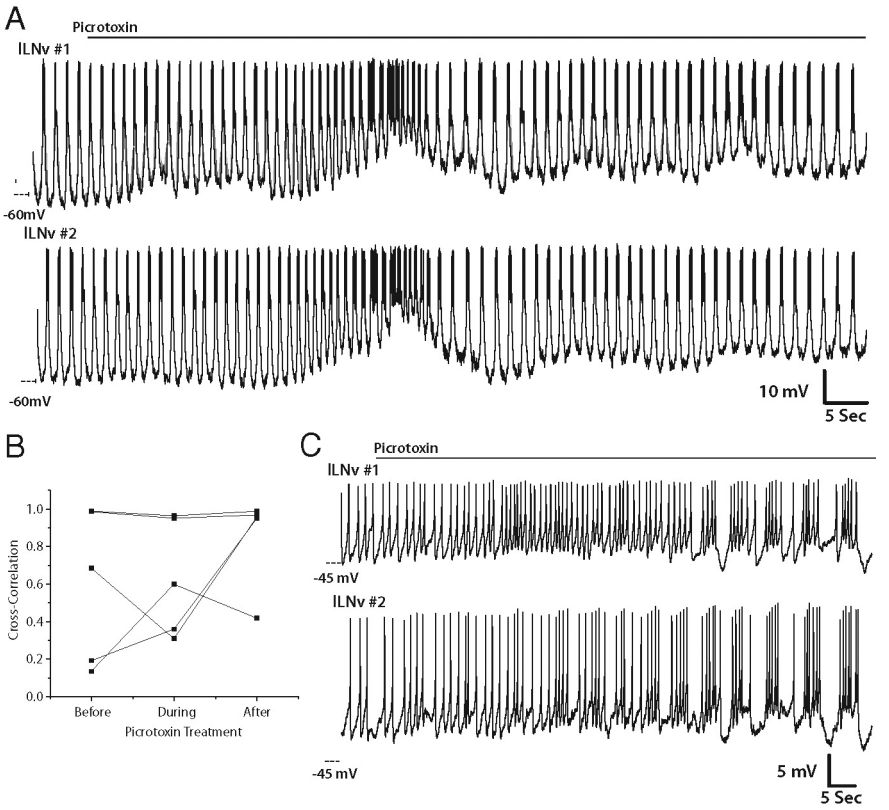

Figure 9. Inhibition of GABAergic inputs does not block lLN_v synchrony but does modulate lLN_v firing pattern. ***A***, Representative simultaneous whole-cell current-clamp recordings of two ipsilateral lLN_vs treated with picrotoxin (100 μM) ($n = 5$). All paired recordings were performed between ZT22 and ZT23. ***B***, Quantification of the correlation of membrane activity between pairs of lLN_vs before, during, and after picrotoxin treatment. Each pair that was treated with picrotoxin is shown ($n = 5$). ***C***, Representative trace of a pair of lLN_vs that switch their mode of firing from tonic to bursting as a result of picrotoxin treatment ($n = 2$).

To characterize the nature of synaptic inputs to lLN_vs, we used a combination of agonists and antagonists against neurotransmitter receptors in both current-clamp and voltage-clamp mode. Current-clamp mode was used to monitor modulation of membrane activity in the lLN_vs in the context of the functional neural network, whereas voltage-clamp mode was used to determine the presence of underlying receptors in the lLN_vs themselves. We found that lLN_vs receive excitatory cholinergic input through nAChR (Figs. 3, 4*D*,*E*). Treatment of brains with cholinergic receptor agonists, acetylcholine and nicotine, enhances membrane activity, depolarizing the neurons and increasing action potential firing rate, whereas treatment with ACh receptor antagonists, curare and α-BuTX, inhibits membrane activity (Fig. 3). Voltage-clamp recordings in the presence of TTX revealed that ACh- and nicotine-induced currents occur in lLN_vs themselves, and these currents reverse near the equilibrium potential for nonselective monovalent cation channels, as expected for currents through nicotinic acetylcholine receptors (Fig. 4*D*,*E*). In insects, acetylcholine is the primary excitatory neurotransmitter in the CNS (Sattelle et al., 1989; Gundelfinger and Hess, 1992), and nAChRs are widely expressed in the *Drosophila* brain (Schuster et al., 1993). These receptors are known to mediate fast synaptic transmission in Kenyon cells in the adult mushroom body (Su and O'Dowd, 2003; Gu and O'Dowd, 2006). A previous study has also shown that dissociated PDF-positive neurons from the larval *Drosophila* brain, which are developmental precursors of the LN_vs, express nAChRs and exhibit both ACh-induced and nicotine-induced increases in intracellular calcium that are dependent on both external sodium and calcium concentrations (Wegener et al., 2004). Our findings confirm that lLN_vs in the adult circadian neural network possess nAChRs and that these receptors mediate excitatory synaptic input and synchrony of rhythmic firing.

GABA is a major neurotransmitter in the *Drosophila* CNS (ffrench-Constant et al., 1991), mediating fast inhibitory synaptic transmission through the $GABA_A$ receptor. This receptor has been shown to be expressed in LN_vs and has been shown genetically to play a major role in the regulation of arousal and sleep by lLN_vs specifically (Parisky et al., 2008; Shang et al., 2008; Chung et al., 2009). GABA-induced decreases in intracellular calcium and Cl^- currents have been recorded in dissociated PDF neurons from the larval and adult fly brain, respectively (Hamasaka et al., 2005; Chung et al., 2009), but previous studies have not analyzed effects of GABA on lLN_v membrane activity in the context of the intact circadian rest/arousal control network. We demonstrate that GABA inhibits the membrane activity of lLN_vs, whereas the ionotropic GABAR antagonist, picrotoxin, is excitatory (Fig. 5*A*,*B*,*D*,*E*). In contrast, the study by Hamasaka et al. shows no rescue of the inhibitory effect of GABA by picrotoxin on PDF+ LN_v precursors (Hamasaka et al., 2005) but does show alleviation of GABA-induced inhibitory responses in these neurons by metabotropic $GABA_BR$ antagonists. Although our studies do not exclude a role for $GABA_B$Rs in lLN_vs, the discrepancy of the effect of picrotoxin could be attributable to changes in different GABAR subtype expression at different developmental stages.

Through an extensive series of voltage-clamp experiments we determined that GABA induces currents in lLN_vs that reverse at

the equilibrium potential of Cl^-, indicating that these currents are mediated by $GABA_A$Rs (Fig. 5*C*). These data demonstrate that lLN_vs express the $GABA_A$R and that lLN_vs receive GABAergic inhibitory synaptic input. Our data from paired recordings in lLN_vs show that GABAergic synaptic input, in conjunction with PDF signaling, plays a critical role in modulating the membrane activity of lLN_vs (Fig. 9*C*) but is not required for the robust synchrony of firing in these neurons, as application of picrotoxin does not abolish synchronous firing (Fig. 9). Conversely, in the cockroach, picrotoxin leads to desynchrony within circadian neural networks (Schneider and Stengl, 2005). In this system, PDF also serves to synchronize these neural populations by inhibiting GABAergic interneurons (Schneider and Stengl, 2005). This mechanism does not seem to be conserved in *Drosophila*, but additional experiments are needed to elucidate the effect of PDF on the synchronous electrical activity of the circadian neural circuit.

Glutamate and its excitatory ionotropic receptors, homologs of the AMPA, kainate, and NMDA receptors in mammals, have been shown to mediate fast excitatory neurotransmission at the neuromuscular junction (NMJ) in *Drosophila* (Jan and Jan, 1976; Ultsch et al., 1992, 1993; Schuster et al., 1993; Littleton and Ganetzky, 2000; Völkner et al., 2000). Interestingly, our data demonstrate that treatment of lLN_vs with glutamate led to an inhibition of membrane activity (Fig. 6*A*), which is opposite to the effect seen at the NMJ. Through voltage-clamp experiments, we show that this glutamate-induced current in lLN_vs reverses near the equilibrium potential of Cl^- (Fig. 6*C*). Furthermore, when we altered the Cl^- concentration of the external solution and measured the reversal potential of the current, the experimental value was well predicted by the calculated equilibrium potential for each specific Cl^- concentration (Fig. 6*C*,*D*). These data together indicate that lLN_vs possess a glutamate-gated Cl^- channel. Members of the GluCl family have been cloned from both *Drosophila* and *C. elegans* (Cully et al., 1994, 1996; Vassilatis et al., 1997) but have not been found in vertebrate species. Their functional roles in neural circuits in *Drosophila* remain enigmatic. Our studies indicate these channels are present in lLN_vs, which also express metabotropic glutamate receptors (Hamasaka et al., 2007). Their role in synchronous membrane activity between lLN_vs remains to be elucidated.

Given the variety of the synaptic inputs to lLN_vs described here, the ability of lLN_vs to autonomously detect light through the blue light-activated photopigment CRY, and the convergence of the arousal and circadian circuits on lLN_vs, these neurons are clearly in a position to integrate complicated signals from all these systems. Our data also show that the rhythmic oscillation in membrane activity seen in these neurons is most likely not attributable to intrinsic pacemaking, but instead arises from synchronized synaptic inputs, both excitatory and inhibitory. It remains to be determined where these cholinergic, GABAergic, and glutamatergic synaptic inputs converging on lLN_vs originate. Previous studies have demonstrated that the Hofbauer–Büchner adult eyelets, which are derived developmentally from Bolwig's organ in the larvae, send axon bundles to the dendritic region on LN_vs (Helfrich-Förster et al., 2002). These cholinergic neurons may provide excitatory input to lLN_vs via nAChRs (Yasuyama et al., 1995; Yasuyama and Salvaterra, 1999; Helfrich-Förster et al., 2002). However, we do not consider it likely that Hofbauer–Büchner cholinergic inputs to the lLN_vs contribute to rhythmic activity in the whole-brain explant. As far as anatomical characterization of the inhibitory inputs into lLN_vs, varicosities in the accessory medulla, which abut lLN_v dendrites, express glutamic acid decarboxylase, a marker for GABAergic neurons (Chung et al., 2009); however, it is not known where cell bodies reside from which these processes originate. In addition, it has been previously shown that other circadian clock neurons are glutamatergic (Hamasaka et al., 2007; Daniels et al., 2008). The axon terminals of these neurons are in close proximity to the dendritic arbors of the lLN_vs in the larval optic center and in the accessory medulla of the adult fly (Hamasaka et al., 2007; Daniels et al., 2008). These data, in combination with our findings, suggest that GluCl within lLN_vs may mediate inhibitory synaptic inputs from other clock neurons in the circadian circuit.

Through the use of whole-cell patch-clamp electrophysiology techniques, we have demonstrated synchronous membrane activity of lLN_vs of the circadian rest/arousal neural network of *Drosophila* arising from bilateral synchronized synaptic inputs. This synchronous membrane activity is mediated by cholinergic inputs to the lLN_vs themselves (Fig. 7). However, GABAergic inputs modulate membrane activity of these neurons but are not required for synchrony (Fig. 9). The role of glutamatergic signaling in synchronous membrane activity between lLN_v pairs remains to be revealed, as agents to pharmacologically inhibit GluCl are not currently available. Building on these findings, future studies are required to elucidate the overlapping neural circuitry of the circadian, rest/arousal, and light input systems, and will discern how these systems are integrated and finely coordinated to generate a robust and complex pattern of behavior.

References

Albus H, Vansteensel MJ, Michel S, Block GD, Meijer JH (2005) A GABAergic mechanism is necessary for coupling dissociable ventral and dorsal regional oscillators within the circadian clock. Curr Biol 15:886–893.

Aronstein K, ffrench-Constant R (1995) Immunocytochemistry of a novel GABA receptor subunit Rdl in *Drosophila melanogaster*. Invert Neurosci 1:25–31.

Aton SJ, Colwell CS, Harmar AJ, Waschek J, Herzog ED (2005) Vasoactive intestinal polypeptide mediates circadian rhythmicity and synchrony in mammalian clock neurons. Nat Neurosci 8:476–483.

Aton SJ, Huettner JE, Straume M, Herzog ED (2006) GABA and Gi/o differentially control circadian rhythms and synchrony in clock neurons. Proc Natl Acad Sci U S A 103:19188–19193.

Blake AD, Anthony NM, Chen HH, Harrison JB, Nathanson NM, Sattelle DB (1993) *Drosophila* nervous system muscarinic acetylcholine receptor: transient functional expression and localization by immunocytochemistry. Mol Pharmacol 44:716–724.

Blanchardon E, Grima B, Klarsfeld A, Chélot E, Hardin PE, Préat T, Rouyer F (2001) Defining the role of *Drosophila* lateral neurons in the control of circadian rhythms in motor activity and eclosion by targeted genetic ablation and PERIOD protein overexpression. Eur J Neurosci 13:871–888.

Bossy B, Ballivet M, Spierer P (1988) Conservation of neural nicotinic acetylcholine receptors from *Drosophila* to vertebrate central nervous systems. EMBO J 7:611–618.

Brand AH, Perrimon N (1993) Targeted gene expression as a means of altering cell fates and generating dominant phenotypes. Development 118:401–415.

Cao G, Nitabach MN (2008) Circadian control of membrane excitability in *Drosophila melanogaster* lateral ventral clock neurons. J Neurosci 28:6493–6501.

Chung BY, Kilman VL, Keath JR, Pitman JL, Allada R (2009) The $GABA_A$ receptor RDL acts in peptidergic PDF neurons to promote sleep in *Drosophila*. Curr Biol 19:386–390.

Cirelli C, Bushey D (2008) Sleep and wakefulness in *Drosophila melanogaster*. Ann N Y Acad Sci 1129:323–329.

Collins BH, Dissel S, Gaten E, Rosato E, Kyriacou CP (2005) Disruption of Cryptochrome partially restores circadian rhythmicity to the ar-

rhythmic period mutant of *Drosophila*. Proc Natl Acad Sci U S A 102:19021–19026.
Cook A, Aptel N, Portillo V, Siney E, Sihota R, Holden-Dye L, Wolstenholme A (2006) *Caenorhabditis elegans* ivermectin receptors regulate locomotor behaviour and are functional orthologues of *Haemonchus contortus* receptors. Mol Biochem Parasitol 147:118–125.
Cully DF, Vassilatis DK, Liu KK, Paress PS, Van der Ploeg LH, Schaeffer JM, Arena JP (1994) Cloning of an avermectin-sensitive glutamate-gated chloride channel from *Caenorhabditis elegans*. Nature 371:707–711.
Cully DF, Paress PS, Liu KK, Schaeffer JM, Arena JP (1996) Identification of a *Drosophila melanogaster* glutamate-gated chloride channel sensitive to the antiparasitic agent avermectin. J Biol Chem 271:20187–20191.
Daniels RW, Gelfand MV, Collins CA, DiAntonio A (2008) Visualizing glutamatergic cell bodies and synapses in *Drosophila* larval and adult CNS. J Comp Neurol 508:131–152.
Dent JA, Davis MW, Avery L (1997) avr-15 encodes a chloride channel subunit that mediates inhibitory glutamatergic neurotransmission and ivermectin sensitivity in *Caenorhabditis elegans*. EMBO J 16:5867–5879.
Dent JA, Smith MM, Vassilatis DK, Avery L (2000) The genetics of ivermectin resistance in *Caenorhabditis elegans*. Proc Natl Acad Sci U S A 97:2674–2679.
Dubruille R, Emery P (2008) A plastic clock: how circadian rhythms respond to environmental cues in *Drosophila*. Mol Neurobiol 38:129–145.
ffrench-Constant RH, Mortlock DP, Shaffer CD, MacIntyre RJ, Roush RT (1991) Molecular cloning and transformation of cyclodiene resistance in *Drosophila*: an invertebrate gamma-aminobutyric acid subtype A receptor locus. Proc Natl Acad Sci U S A 88:7209–7213.
Fisahn A (2005) Kainate receptors and rhythmic activity in neuronal networks: hippocampal gamma oscillations as a tool. J Physiol 562:65–72.
Gu H, O'Dowd DK (2006) Cholinergic synaptic transmission in adult *Drosophila* Kenyon cells *in situ*. J Neurosci 26:265–272.
Gundelfinger ED, Hess N (1992) Nicotinic acetylcholine receptors of the central nervous system of *Drosophila*. Biochim Biophys Acta 1137:299–308.
Hamasaka Y, Wegener C, Nässel DR (2005) GABA modulates *Drosophila* circadian clock neurons via GABAB receptors and decreases in calcium. J Neurobiol 65:225–240.
Hamasaka Y, Rieger D, Parmentier ML, Grau Y, Helfrich-Förster C, Nässel DR (2007) Glutamate and its metabotropic receptor in *Drosophila* clock neuron circuits. J Comp Neurol 505:32–45.
Harmar AJ, Marston HM, Shen S, Spratt C, West KM, Sheward WJ, Morrison CF, Dorin JR, Piggins HD, Reubi JC, Kelly JS, Maywood ES, Hastings MH (2002) The $VPAC_2$ receptor is essential for circadian function in the mouse suprachiasmatic nuclei. Cell 109:497–508.
Helfrich-Förster C (2004) The circadian clock in the brain: a structural and functional comparison between mammals and insects. J Comp Physiol A Neuroethol Sens Neural Behav Physiol 190:601–613.
Helfrich-Förster C (2005) Neurobiology of the fruit fly's circadian clock. Genes Brain Behav 4:65–76.
Helfrich-Förster C, Edwards T, Yasuyama K, Wisotzki B, Schneuwly S, Stanewsky R, Meinertzhagen IA, Hofbauer A (2002) The extraretinal eyelet of *Drosophila*: development, ultrastructure, and putative circadian function. J Neurosci 22:9255–9266.
Helfrich-Förster C, Shafer OT, Wülbeck C, Grieshaber E, Rieger D, Taghert P (2007) Development and morphology of the clock-gene-expressing lateral neurons of *Drosophila melanogaster*. J Comp Neurol 500:47–70.
Hosie AM, Aronstein K, Sattelle DB, ffrench-Constant RH (1997) Molecular biology of insect neuronal GABA receptors. Trends Neurosci 20:578–583.
Inouye ST, Kawamura H (1979) Persistence of circadian rhythmicity in a mammalian hypothalamic "island" containing the suprachiasmatic nucleus. Proc Natl Acad Sci U S A 76:5962–5966.
Jan LY, Jan YN (1976) L-glutamate as an excitatory transmitter at the *Drosophila* larval neuromuscular junction. J Physiol 262:215–236.
Kaneko M, Park JH, Cheng Y, Hardin PE, Hall JC (2000) Disruption of synaptic transmission or clock-gene-product oscillations in circadian pacemaker cells of *Drosophila* cause abnormal behavioral rhythms. J Neurobiol 43:207–233.
Laughton DL, Lunt GG, Wolstenholme AJ (1997) Alternative splicing of a *Caenorhabditis elegans* gene produces two novel inhibitory amino acid receptor subunits with identical ligand binding domains but different ion channels. Gene 201:119–125.
Littleton JT, Ganetzky B (2000) Ion channels and synaptic organization: analysis of the *Drosophila* genome. Neuron 26:35–43.
Liu C, Reppert SM (2000) GABA synchronizes clock cells within the suprachiasmatic circadian clock. Neuron 25:123–128.
Maywood ES, Reddy AB, Wong GK, O'Neill JS, O'Brien JA, McMahon DG, Harmar AJ, Okamura H, Hastings MH (2006) Synchronization and maintenance of timekeeping in suprachiasmatic circadian clock cells by neuropeptidergic signaling. Curr Biol 16:599–605.
Mertens I, Husson SJ, Janssen T, Lindemans M, Schoofs L (2007) PACAP and PDF signaling in the regulation of mammalian and insect circadian rhythms. Peptides 28:1775–1783.
Nitabach MN, Taghert PH (2008) Organization of the *Drosophila* circadian control circuit. Curr Biol 18:R84–R93.
Nitabach MN, Blau J, Holmes TC (2002) Electrical silencing of *Drosophila* pacemaker neurons stops the free-running circadian clock. Cell 109:485–495.
Nitabach MN, Wu Y, Sheeba V, Lemon WC, Strumbos J, Zelensky PK, White BH, Holmes TC (2006) Electrical hyperexcitation of lateral ventral pacemaker neurons desynchronizes downstream circadian oscillators in the fly circadian circuit and induces multiple behavioral periods. J Neurosci 26:479–489.
Nitz DA, van Swinderen B, Tononi G, Greenspan RJ (2002) Electrophysiological correlates of rest and activity in *Drosophila melanogaster*. Curr Biol 12:1934–1940.
Parisky KM, Agosto J, Pulver SR, Shang Y, Kuklin E, Hodge JJ, Kang K, Liu X, Garrity PA, Rosbash M, Griffith LC (2008) PDF cells are a GABA-responsive wake-promoting component of the *Drosophila* sleep circuit. Neuron 60:672–682.
Renn SC, Park JH, Rosbash M, Hall JC, Taghert PH (1999) A pdf neuropeptide gene mutation and ablation of PDF neurons each cause severe abnormalities of behavioral circadian rhythms in *Drosophila*. Cell 99:791–802.
Rosay P, Armstrong JD, Wang Z, Kaiser K (2001) Synchronized neural activity in the *Drosophila* memory centers and its modulation by amnesiac. Neuron 30:759–770.
Sattelle DB, Mädler U, Heilgenberg H, Breer H (1989) Immunocytochemical localization of nicotinic acetylcholine receptors in the terminal abdominal ganglion of the cockroach (*Periplaneta americana*). Proc R Soc Lond B Biol Sci 238:189–192.
Schneider NL, Stengl M (2005) Pigment-dispersing factor and GABA synchronize cells of the isolated circadian clock of the cockroach *Leucophaea maderae*. J Neurosci 25:5138–5147.
Schuster CM, Ultsch A, Schloss P, Cox JA, Schmitt B, Betz H (1991) Molecular cloning of an invertebrate glutamate receptor subunit expressed in *Drosophila* muscle. Science 254:112–114.
Schuster R, Phannavong B, Schröder C, Gundelfinger ED (1993) Immunohistochemical localization of a ligand-binding and a structural subunit of nicotinic acetylcholine receptors in the central nervous system of *Drosophila melanogaster*. J Comp Neurol 335:149–162.
Shang Y, Griffith LC, Rosbash M (2008) Light-arousal and circadian photoreception circuits intersect at the large PDF cells of the *Drosophila* brain. Proc Natl Acad Sci U S A 105:19587–19594.
Sheeba V, Gu H, Sharma VK, O'Dowd DK, Holmes TC (2008a) Circadian- and light-dependent regulation of resting membrane potential and spontaneous action potential firing of *Drosophila* circadian pacemaker neurons. J Neurophysiol 99:976–988.
Sheeba V, Fogle KJ, Kaneko M, Rashid S, Chou YT, Sharma VK, Holmes TC (2008b) Large ventral lateral neurons modulate arousal and sleep in *Drosophila*. Curr Biol 18:1537–1545.
Shirakawa T, Honma S, Katsuno Y, Oguchi H, Honma KI (2000) Synchronization of circadian firing rhythms in cultured rat suprachiasmatic neurons. Eur J Neurosci 12:2833–2838.
Su H, O'Dowd DK (2003) Fast synaptic currents in *Drosophila* mushroom body Kenyon cells are mediated by α-bungarotoxin-sensitive nicotinic acetylcholine receptors and picrotoxin-sensitive GABA receptors. J Neurosci 23:9246–9253.
Ultsch A, Schuster CM, Laube B, Schloss P, Schmitt B, Betz H (1992) Glutamate receptors of *Drosophila melanogaster*: cloning of a kainate-selective subunit expressed in the central nervous system. Proc Natl Acad Sci U S A 89:10484–10488.
Ultsch A, Schuster CM, Laube B, Betz H, Schmitt B (1993) Glutamate receptors of *Drosophila melanogaster*. Primary structure of a putative

NMDA receptor protein expressed in the head of the adult fly. FEBS Lett 324:171–177.

Vassilatis DK, Arena JP, Plasterk RH, Wilkinson HA, Schaeffer JM, Cully DF, Van der Ploeg LH (1997) Genetic and biochemical evidence for a novel avermectin-sensitive chloride channel in *Caenorhabditis elegans*. Isolation and characterization. J Biol Chem 272:33167–33174.

Völkner M, Lenz-Böhme B, Betz H, Schmitt B (2000) Novel CNS glutamate receptor subunit genes of *Drosophila melanogaster*. J Neurochem 75:1791–1799.

Wagner S, Castel M, Gainer H, Yarom Y (1997) GABA in the mammalian suprachiasmatic nucleus and its role in diurnal rhythmicity. Nature 387:598–603.

Wegener C, Hamasaka Y, Nässel DR (2004) Acetylcholine increases intracellular Ca^{2+} via nicotinic receptors in cultured PDF-containing clock neurons of *Drosophila*. J Neurophysiol 91:912–923.

Welsh DK, Logothetis DE, Meister M, Reppert SM (1995) Individual neurons dissociated from rat suprachiasmatic nucleus express independently phased circadian firing rhythms. Neuron 14:697–706.

Welsh DK, Takahashi JS, Kay SA (2010) Suprachiasmatic nucleus: cell autonomy and network properties. Annu Rev Physiol 72:551–577.

Wu Y, Cao G, Nitabach MN (2008a) Electrical silencing of PDF neurons advances the phase of non-PDF clock neurons in *Drosophila*. J Biol Rhythms 23:117–128.

Wu Y, Cao G, Pavlicek B, Luo X, Nitabach MN (2008b) Phase coupling of a circadian neuropeptide with rest/activity rhythms detected using a membrane-tethered spider toxin. PLoS Biol 6:e273.

Yasuyama K, Salvaterra PM (1999) Localization of choline acetyltransferase-expressing neurons in *Drosophila* nervous system. Microsc Res Tech 45:65–79.

Yasuyama K, Kitamoto T, Salvaterra PM (1995) Localization of choline acetyltransferase-expressing neurons in the larval visual system of *Drosophila melanogaster*. Cell Tissue Res 282:193–202.